Pergamon

Bioorganic & Medicinal Chemistry 7 (1999) 359–367

BIOORGANIC & MEDICINAL CHEMISTRY

A New Antioxidative Vitamin B_6 Analogue Modulates Pathophysiological Cell Proliferation and Damage

Andreas J. Kesel,[a] Isolde Sonnenbichler,[a] Kurt Polborn,[b] Lutz Gürtler,[c] Wolfgang E. F. Klinkert,[d] Manuel Modolell,[e] Andreas K. Nüssler[f] and Walter Oberthür[a,*]

[a]*Max-Planck-Institut für Biochemie, D-82152 Martinsried, Germany*
[b]*Institut für Organische Chemie der Universität München, D-80333 München, Germany*
[c]*Max von Pettenkofer-Institut für Hygiene und Medizinische Mikrobiologie der Universität München, D-80336 München, Germany*
[d]*Max-Planck-Institut für Neurobiologie, D-82152 Martinsried, Germany*
[e]*Max-Planck-Institut für Immunbiologie, D-79108 Freiburg, Germany*
[f]*Chirurgische Klinik der Universität Ulm, D-89073 Ulm, Germany*

Received 9 October 1998

Abstract—The new large scale synthesis of the yellow colored vitamin B_6 analogue 5′-*O*-phosphono-pyridoxylidenerhodanine (**2**) (B6PR) leads to oligohydrates of its monosodium salt (**4**). The light-red hemiheptadecahydrate (8½ hydrate) (**4a**) was crystallized and its three-dimensional structure determined by X-ray crystallography. Special nucleotide and protein interaction properties together with scavenging antioxidative function are combined in this simple water-soluble vitamin B_6 analogues B6PR. High (mM) concentrations were untoxic to 'healthy' not affected cells and primary tissues. Complexation of ions (e.g. Ca^{2+}, Fe^{2+}, and Zn^{2+}), modulation of nitric oxide synthases (NOS I-III), nitric oxide (NO) metabolism, and reactive oxygen species (ROS) was found. Special cytoprotecting, immunomodulating, stimulating and inhibiting activities were observed in vitro, not in comparison with some natural and synthetic pyridoxines. Low B6PR suppressed proliferation, high induced selective cell death of some cancer cell lines. Low B6PR protected HIV-1-infected $CD4^+$ HUT 78 cells against HIV-1-mediated destruction (complete inhibition of HIV-1-induced syncytia formation and cell death) and reduced p24 level. Autoreactive S100β-specific T cells of Lewis rat, a model of multiple sclerosis, could be influenced. Oxidative damage and age, acquired and inherited disease related pathophysiological disorders can be treated by this new cytopathology-selective versatile acting B6PR.

Introduction

Between the years 1934 and 1936 Paul György identified a water-soluble factor curing dermatitis of selectively fed rats, and named it vitamin B_6,[1a,b] since 1939 cited as pyridoxine(s) (Fig. 1(a)). Acting in enzyme-bound (coenzyme function) and free form, pyridoxines are biocatalytically involved in most of biochemical, (cell-) physiological centers and intermediary metabolism of living. In former times a lot of analogues were designed to influence this diverse biological and biochemical systems.[1c] Inspired by the reagent *p*-dimethylaminobenzalrhodanine introduced by Feigl[2] for the detection of silver, Escobar Godoy and Guiraúm Pérez[3] observed a *Knoevenagel* condensation of pyridoxal with rhodanine. They found the pyridoxal analogue pyridoxylidenerhodanine or 5-[[3-hydroxy-5-(hydroxymethyl)-2-methyl-4-pyridinyl]methylene]-2-thioxo-4-thiazolidinone (**1**)[3] to be suitable for the spectrophotometric quantification of silver. These results stimulated our efforts to construct the pyridoxal 5′-phosphate analogue B6PR[4,5] (Fig. 1(b)) 5′-*O*-phosphono-pyridoxylidenerhodanine or 5-[[5-hydroxy-6-methyl-3-[(phosphonooxy)methyl]-4-pyridinyl]methylene]-2-thioxo-4-thiazolidinone and to examine its function and biological activities.

Results and Discussion

Synthesis

A new large-scale simple synthesis, *Knoevenagel* condensation of pyridoxal 5′-phosphate with rhodanine (2-thioxo-4-thiazolidinone), leads in high yield to water-soluble fluorescent and colored three forms of B6PR: a yellow free acid **2**, and two different monosodium salts [a light red (*Z*)-B6PRNa hemiheptadecahydrate

Key words: Nitric oxide synthase; multiple sclerosis; HIV/AIDS; cancer; inflammation/sepsis.
*Corresponding author. Tel: +49-8166-7830; fax: +49-8166-68111; e-mail: oberthue@biochem.mpg.de

0968-0896/99/$ - see front matter
PII: S0968-0896(98)00229-6

(8½ hydrate) **4a** and a dark red compound, probably (*Z*)-B6PRNa hemipentahydrate (2½ hydrate) **4b**]. Chemistry is summarized in the experimental section.

Resolution of the three-dimensional structure of 4a

The monosodium salt **4a** was crystallized as light-red monoclinic plates with the space group C2/c. The crystal structure was determined by X-ray crystallography[6] and found to be (*Z*)-B6PRNa, 8½ hydrate (Fig. 2(a,b)).

Characterization of B6PR

B6PR (all three forms) shows multiple physicochemical properties that have been analyzed. Aggregation to 'self-assembled polymers', complexation of mono- and polyvalent ions (e.g. high affinity binding of Ca^{2+}, Fe^{2+}, and Zn^{2+}) (Fig. 3), reaction with radicals under changing of color created by adding hydrogen peroxide (H_2O_2) or ammonium peroxydisulfate [$(NH_4)_2S_2O_8$], reversible photochemical interconversion of *Z*- and *E*-isomers (Figs 4 and 5), photochemical reactivity etc. were observed. In Figure 5 an improved interpretation of the intramolecular tautomerism and the stereoisomerism of B6PR (5′-*O*-phosphono-pyridoxylidene-rhodanine) is proposed in addition to irradiation decomposition products **1** and **7**.

Biological activities

The physicochemical properties and the assumed interactions of B6PR with DNA/RNA[4] (Fig. 1(b)) and proteins lead to predictions and experiments with cell culture systems. No cytopathic effect was observed with range ng mL^{-1} to mg mL^{-1} **4a** and **4b** to not affected primary avian sympathetic neurons and normal rodent T cells, cultured under physiological conditions. The growth of *Dictyostelium discoideum* cells in axenic medium was not influenced, expression of untoxic behaviour of (*Z*)-B6PR to different primary cell types.

Next we examined the effect of low and high light red (*Z*)-B6PR to malignant $CD4^+$ HUT 78 cutaneous T lymphoma cells[7] in comparison with HIV-1-infected HUT 78 cells. In the low concentration (1 μg mL^{-1}) **4a** completely abolished syncytia formation and cytopathic changes of all HIV-1-infected HUT 78 cells without being toxic to the uninfected host cell. In the MTT mitochondrial viability assay,[8] a measurement for life of

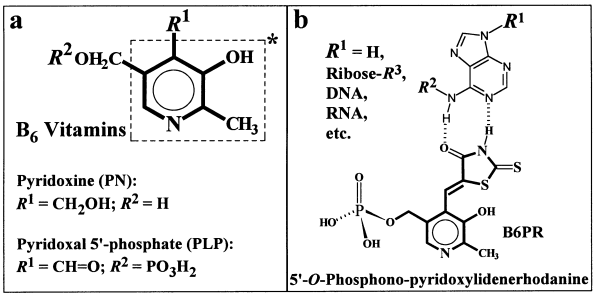

Figure 1. Structure of natural pyridoxines and the synthetic analogue B6PR. (a) Lead structure* [5(3)-hydroxy-6(2)-methylpyridine] of the vitamin B_6 group, cited as pyridoxines according to the B_6 vitamin pyridoxine; the substituents of pyridoxine and the main important B_6 vitamin pyridoxal 5′-phosphate. (b) The structure of vitamin B_6 analogue B6PR (5′-*O*-phosphono-pyridoxylidenerhodanine), able to bind to various adenine-containing targets like adenosine, AMP, ADP, ATP, NAD^+, $NADP^+$, RNA, DNA, plant hormones (zeatin, kinetin), oligonucleotides etc.

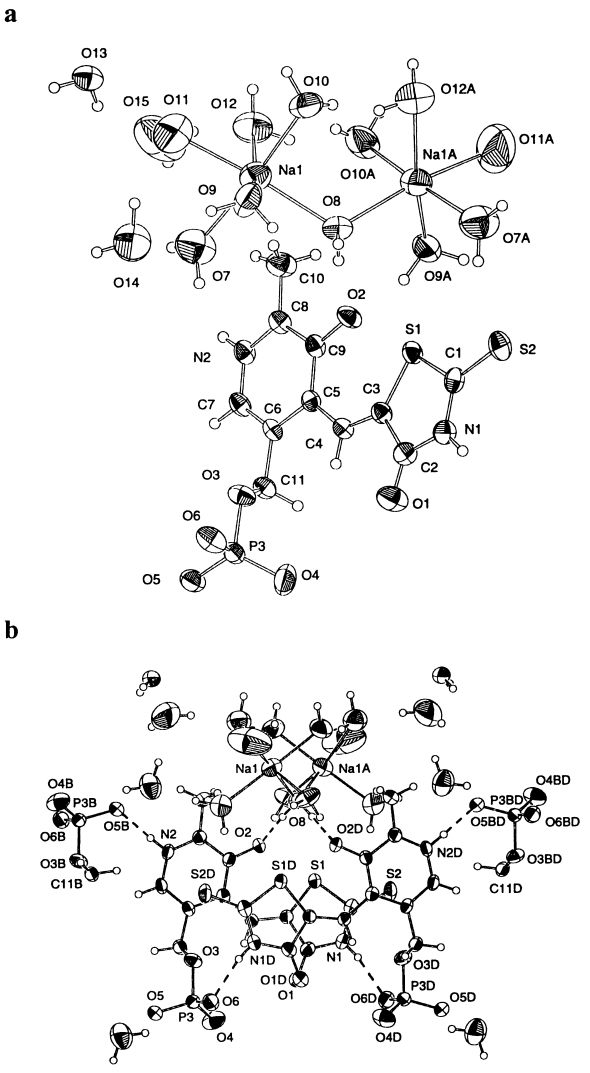

Figure 2. (a) Structure of **4a** in the crystal. (b) Plot of the dimeric **4a** in the crystal.

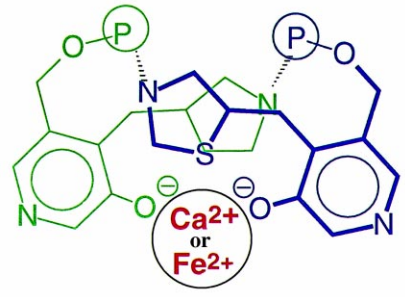

Figure 3. The cation binding (chelating function) of (*Z*)-B6PR at physiological pH, high affinity binding of, for example, Ca^{2+}, Fe^{2+}, and Zn^{2+} was found.

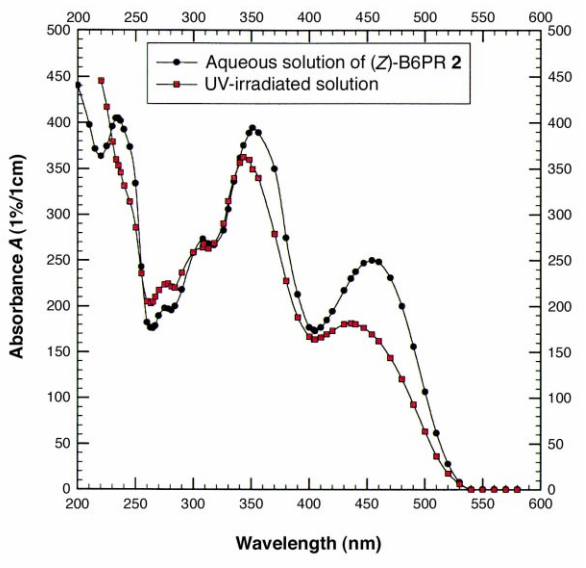

Figure 4. UV/VIS spectra in H_2O of (*Z*)-isomer **2** before and after 1 h low energy UV-B irradiation (312 nm), leading to the (*E*)-isomer **3**. Back-rearrangement to (*Z*)-isomer **2** was observed 33 h later. ^1H NMR control of this experiment in D_2O and TLC pointed to no other chemical change in the molecule.

cells, low **4a** completely antagonized HIV-1-induced cytopathic effect and cell death (Fig. 6). Virus entry, replication and release in HUT 78 cells as measured by p24 (the viral core protein) level in the supernatant[9] at day six is not inhibited by designated low B6PR concentration, in contrary with 10 μg mL^{-1} (42% reduction of p24 level, data not shown). But HIV-1-infected and producing HUT 78 cells are completely 'healthy', not inhibited in their function and proliferation, which was never observed before in this test system. Interestingly, applied in the concentration 100 μg mL^{-1} and higher **4a** also abolished syncytia formation and in addition no p24 could be detected. But also cell death of unchanged infected cells between day 3 and 4 after infection was observed, induced evidently by the effect of B6PR to the malignant host cell line itself, found also in the uninfected cell control.

We therefore examined different malignant cell lines, to get more information about general B6PR anticancer activity. A great variety of human immortalized cancer cell lines showed even in lowest or lower concentrations (5.3 ng mL^{-1} to 53.7 μg mL^{-1}) of **4a** a concentration and cell line dependent suppression or complete inhibition

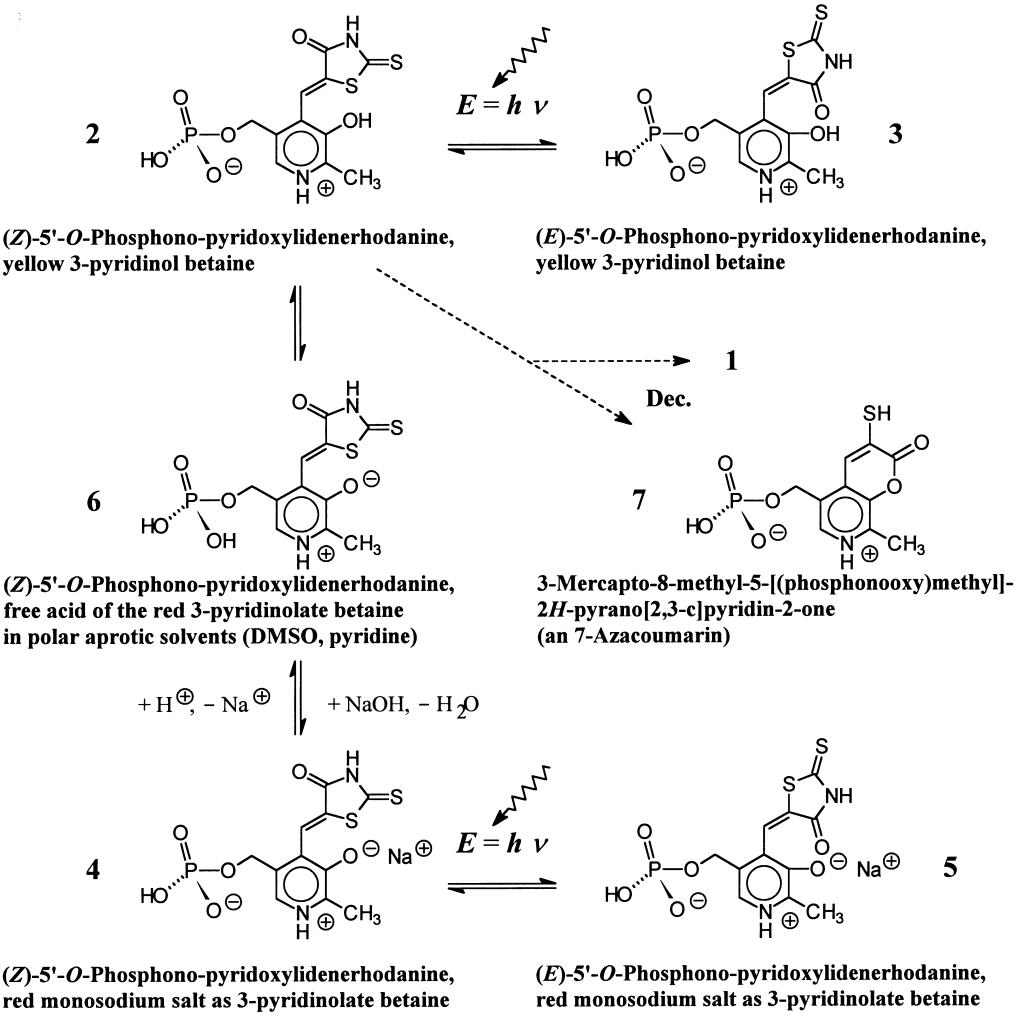

Figure 5. Proposed stereoisomerism, tautomerism of **2**, decomposition products **1** and **7** following long time irradiation of **2**.

of proliferation (Fig. 7). But also activation, no influence and differences in two test series were observed. The murine tumor cell line Abelson 8.1 of pre-B lymphoid lineage,[10,11] which was highly suppressed or completely killed at higher concentration (250 μg mL^{-1}) of **4a** and **4b** (data not shown), was used to compare acting of (*Z*)-B6PRNa with other pyridoxines. No or low influence in the same concentrations by natural pyridoxines, some synthetic derivatives and astonishingly **1** were observed.

The difference in the sensitivity of various primary and malignant cells to B6PR reflects a special feature, known from phosphorylated pyridoxines, which cannot pass intact cell membrane. Transport mechanism was shown to be passive diffusion of dephosphorylated forms and 'metabolic trapping' inside/outside the cell due to de-/rephosphorylation. Some cancer cells intrinsically express different levels of signal peptide-addressed membrane-anchored alkaline phosphatase including Abelson 8.1,[10,11] or acidic phosphatase like HUT 78.[7] Dephosphorylation of the pro-drug fosfestrol (diethylstilbestrol diphosphate)[12a] on the cell surface yielded diethylstilbestrol[12b] which invades the malignant prostatic cell and is enriched in it and there exerts estrogenic-induced cytostasis[12c,d] or apoptosis.[12e] We assume the same cytopathology-selective cell invasion of B6PR into tumor tissue by this highly unspecific phosphatases. However, mechanisms of invasion and acting remain open and should be further examined.

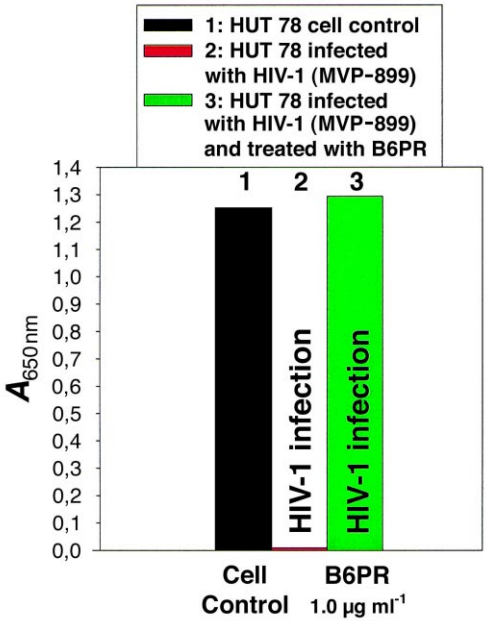

Figure 6. MTT mitochondrial viability test for determination of HIV-1-induced (laboratory-adapted T-tropic SI HIV-1 subtype B strain MVP-899) cytopathic effect on human $CD4^+$ HUT 78 cutaneous T lymphoma cells in the absence or presence of infection at day 0 and with or without previous adding of **4a**. In the middle bar 2 all HIV-1-infected cells are destroyed without B6PR (with previous syncytia formation), in comparison with bar 3 all cells are alive in presence of B6PR (no syncytia formation).

The HIV-induced syncytia formation, the involvement in the depletion of $CD4^+$ T cells during progression of AIDS is unclear and in controversal discussion.[13] It is known that iNOS (inducible type II form of NOS), NO and ROS metabolism are implicated in cell adhesion, chemotaxis, and cell death (e.g. apoptosis).[14] For both steps of (MVP-899) HIV-1-induced HUT 78 $CD4^+$ cell damage 1) syncytia formation and, later, 2) cell death, we assumed an involvement of the nitric oxide synthases.[15] In addition to this proposal we have noticed a similarity of B6PR with L-thiocitrulline,[16] a competitive heme-binding NOS inhibitor (Fig. 8). We examined the effect of B6PR to recombinant NOS isoenzymes of transfected lysed CHO cells. **4a** and **4b** are both slightly different moderate inhibitors[17a] of NOS I-III as measured by conversion of [^{3}H]-L-arginine to [^{3}H]-L-citrulline (50% inhibitory concentrations between 20 μg mL^{-1} and 30 μg mL^{-1}),[17b,c] similar to those obtained with NOS from other species.

To test whether the observed NOS inhibition resulted in a reduced level of reaction products of NO we analysed stimulated cultured murine bone marrow-derived macrophages (BMMØ)[10] and primary rodent hepatocytes as

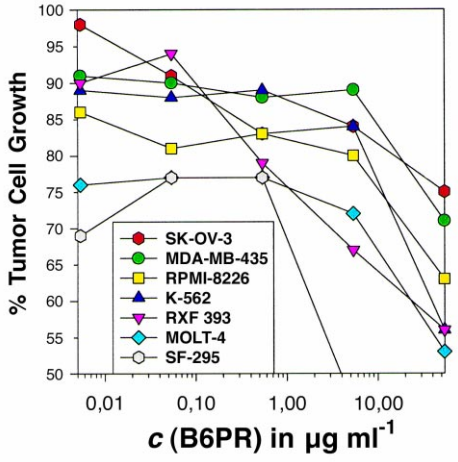

Figure 7. Selection of some human cancer cell lines inhibited by **4a**. Concentration dependent growth suppression (growth with B6PR compared to 100% without) of the leukemia cell lines MOLT-4, RPMI-8226, K-562, the renal cancer cell line RXF 393, the breast cancer cell line MDA-MB-435, the ovarian cancer cell line SK-OV-3, and the glioblastoma tumor cell line SF-295 by B6PR in concentrations ranging from 5.3 ng mL^{-1} to 53.7 μg mL^{-1}.

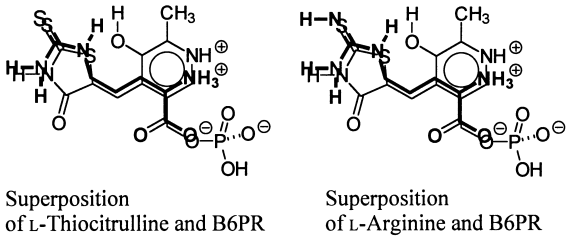

Figure 8. Comparison of B6PR with the competitive NOS I-II inhibitor L-thiocitrulline and the NOS substrate L-arginine.

model of inflammatory events (e.g. sepsis).[18] The nitrite level in the supernatant of BMMØ indicated a poor interference and a concentration dependent reduction. Not more than 15/16% in 24/48 h with low (53 μg mL^{-1}) **4b** (Fig. 9), even in presence of higher (250 μg mL^{-1}) 28/38% in 24/48 h reduction were observed. In the rodent primary hepatocyte culture system, containing low (53 μg mL^{-1}) **4b**, 45% (24 h) reduction of *S*-nitrosothiols[18,19] and nitrite[18,19] (data not shown) in comparison with BMMØ 15% was detected, probably due to the different invasion and acting.

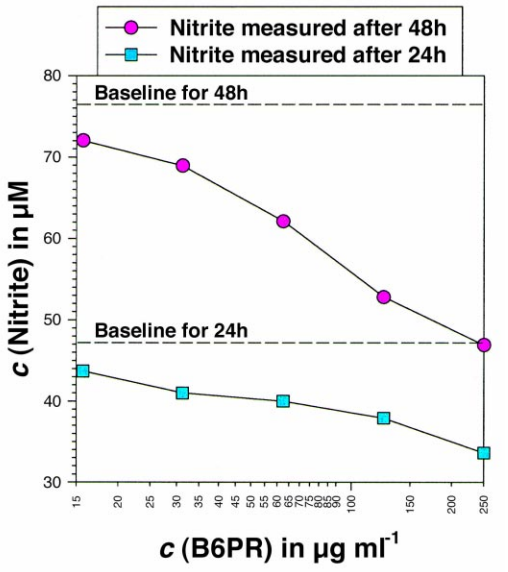

Figure 9. The nitrite level in the culture medium, produced by stimulated [0.1 μg mL^{-1} bacterial lipopolysaccharide (LPS) and 20 U mL^{-1} interferon-γ (IFN-γ)] murine bone marrow-derived macrophages (BMMØ) in 24 and 48 h. Concentration dependent modulation by **4b** indicates 7/15/28% (24 h) and 6/16/38% (48 h) reduction in the presence of 15/53/250 μg mL^{-1}, respectively.

NO is known to inhibit apoptosis and act cell-protective in general, for example by inhibiting lipid peroxidation and terminating free radical chains.[20,21] Preceded by reactive action of highly produced NO or absence of protective level of NO, reactive oxygen species (ROS) are elevated and both induce apoptosis. The level of reaction products of singlet oxygen from NO/hydrogen peroxide, and peroxynitrite from NO/superoxide anion systems[20,21] (leading to DNA damage like strand breaks, consecutive p53 induction and caspase activation) was shown with both cell lines to be significantly reduced by B6PR. The same capacity of **1**, **4a**, and **4b** to react with ROS (·NO and ·OH) in the range of glutathione (GSH) and vitamin C could be confirmed in a special chemical test system (data not shown),[21] nevertheless, the reactivity and specifity towards ·NO and ·OH is identical by **4a** and **4b**, but differently exerted by its dephosphorylated form **1**.

NOS/ROS have been linked with inflammation, septic shock, a number of immunological and neurodegenerative diseases such as multiple sclerosis (MS).[14,21–24] We examined in the experimental autoimmune panencephalitis (EAP) of Lewis rats (animal model of MS) the effect of **4a** and **4b** to pathogenic encephalitogenic S100β-specific T cell clone interaction, which cause inflammatory lesions in the eye and nervous system, not in peripheral S100β containing tissues.[24,25] S100β is one of the most abundant calcium binding proteins in the central nervous system, but is also expressed by many different cell types in a variety of peripheral tissues and in the immune system of humans. Slightly different activities of **4a** and **4b**, a concentration dependent inhibition with low (1–6 μg mL^{-1}) and stimulation with higher (11–100 μg mL^{-1}) of only the S100β-specific T cell clone (Fig. 10(a)) give evidence to influence cell adhesion, autoreactivity, inflammatory cell damage, apoptosis and lesions in human MS. Only poor influence

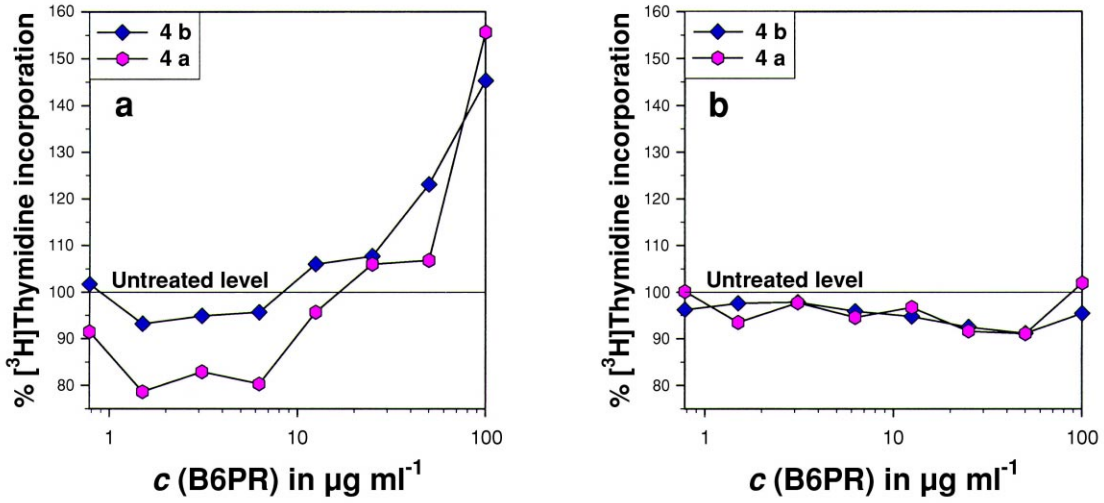

Figure 10. Selective, concentration dependent modulation of one S100β T cell clone interaction and proliferation (immunomodulation) by **4a** and **4b** in comparison with a myelin basic protein (MBP)-specific T cell clone in the experimental autoimmune panencephalitis (EAP) multiple sclerosis S100β-specific non-myelopathic Lewis rat model. (a) One S100β autoreactive encephalitogenic $CD4^+$ TCRαβ T cell clone, Th 1-type lymphocytes, re-stimulated by S100β protein, using irradiated syngeneic thymus cells as source of antigen presenting cells, is inhibited with low (1–6 μg mL^{-1}) and stimulated with higher (11–100 μg mL^{-1}) B6PR. (b) Very poor influence to MBP-specific T cell clone interaction and proliferation.

to myelin basic protein (MBP)-specific T cell clone interaction and proliferation was observed (Fig. 10(b)).

Conclusion

In this paper we have presented a new large scale synthesis of **2** and **4**, as well as characterization (X-ray structure of **4a**), some physicochemical properties, and biological activities of B6PR. This new untoxic vitamin B_6 analogue B6PR, probably a natural compound in plants, combining multiple properties and acting (Fig. 11), should be the first choice for in vivo testing. Its chemotherapeutical potential, reported here for the first time, to modulate oxidative stress, pathophysiological cell proliferation, and cell damage is very important in

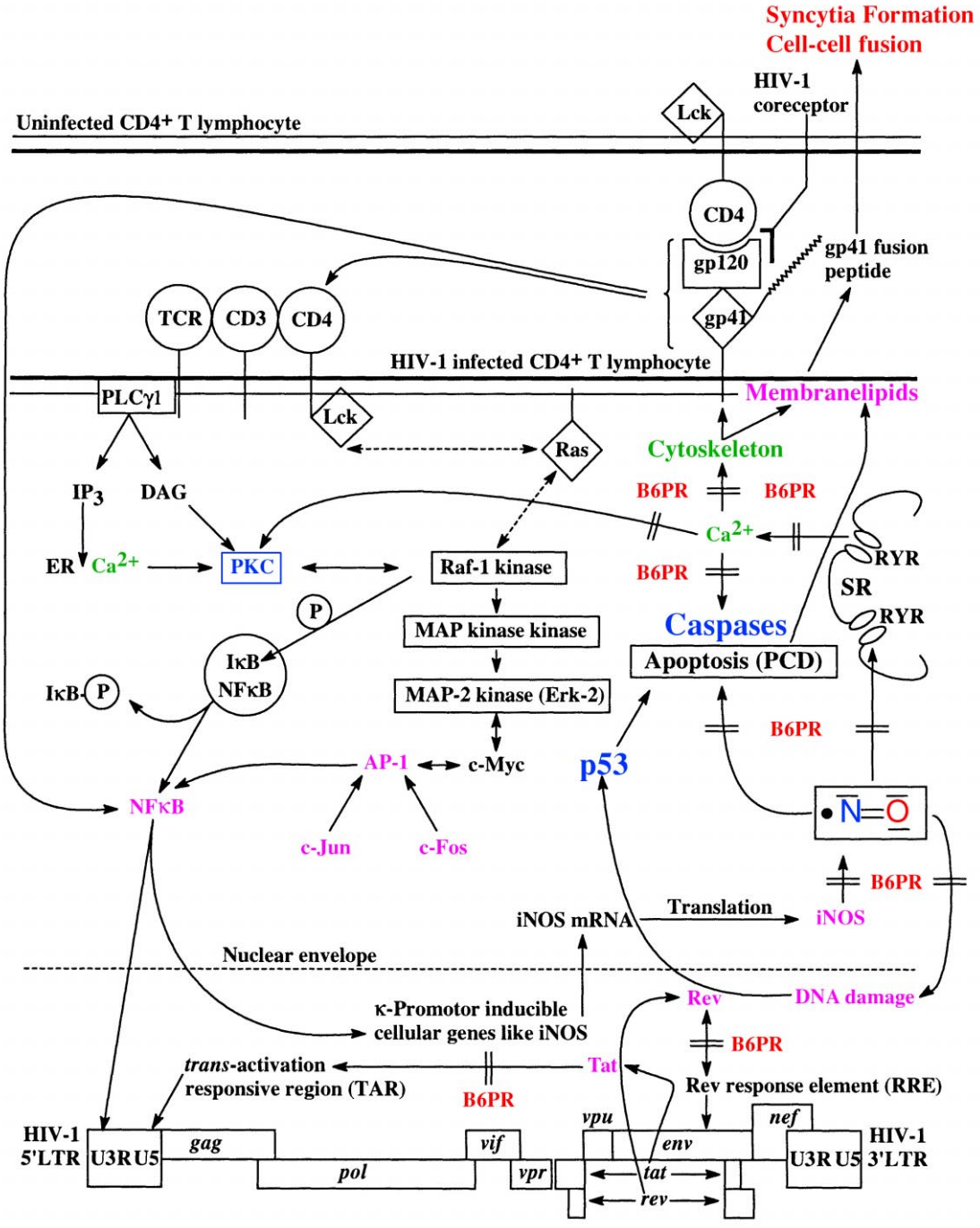

Figure 11. Proposed multiple acting of B6PR in HIV-1-infected $CD4^+$ T lymphocyte (e.g. HUT 78). Abbreviations are CD: cluster of differentiation; TCR/CD3: T cell receptor associated with CD3 complex; Lck: $p56^{lck}$; PLCγ1: phospholipase C γ1; DAG: *sn*-1,2-*O*-diacylglycerol; IP_3: inositol-1,4,5-trisphosphate; PKC: protein kinase C; Ras: $p21^{ras}$; MAP kinase: mitogen-activated protein kinase; ERK: extracellular signal regulated kinase; c-Myc: cellular Myc protein; AP-1: cellular transcription factor AP-1; c-Jun: cellular Jun protein; c-Fos: cellular Fos protein; IκB: inhibitor protein κB; NFκB: nuclear factor κB; LTR: long terminal repeat; ER: endoplasmatic reticulum; SR: sarcoplasmatic reticulum like organelle (microsome); RYR: ryanodine receptor Ca^{2+} channel complex; iNOS: inducible nitric oxide synthase, NOS II.

acquired, inherited, and age related degenerative diseases. The significant connection between the down-regulation of NOS/NO/ROS metabolism by B6PR and biological activities in models of cancer, HIV/AIDS, inflammation and multiple sclerosis, pointed out a correlation, but must be examined further in detail. The elucidation of its multiple mechanisms and application in therapy should be a forcing challenge for the future. It should be discussed, if the specific inhibition/stimulation of only one key molecule (e.g. enzyme, receptor) can be the solitary therapeutical approach (loss of/gain of monospecific intervention), or should be questioned and revised. It should be supplemented by new principles such as maintaining homeostasis or stimulating recovery with untoxic polyspecific drugs like B6PR (a multiplex buffer molecule) or other derivatives with this lead structure (Fig. 12). We know and can learn from NO metabolism cellphysiological homeostasis is important. This work should underline the possibilities of multiple acting B_6 vitamins and their analogues, to protect, keep and reach balance. Their therapeutical use, however, seems to have been overlooked and underestimated and, therefore, may be re-examined and should nowadays be renewed.

Experimental

Melting points were determined in open capillary tubes with a Büchi 510 melting point apparatus. They are uncorrected, occurred only at rapid heating, and could be observed as decomposition intervals. ^{1}H NMR spectra were recorded at 400 MHz and ^{13}C NMR spectra were recorded at 100 MHz on a Bruker AM-400 Fourier transform spectrometer. Internal standards for DMSO-d_6 and pyridine-d_5 were the tabulated solvent signals. The external standard for the measurements in D_2O was the monosodium salt of 3-(trimethylsilyl)-propionic acid-d_4. Chemical shifts are reported in parts per million (δ) in relation to the standard. UV/VIS spectra were recorded in wavelength scan mode on a Beckman DU® 640 spectrophotometer and a Perkin–Elmer Lambda® 20 spectrophotometer at room temperature. Fluorescence excitation and emission spectra were recorded at room temperature using an Aminco Bowman AB2 luminescence spectrophotometer (SLM, Urbana, IL, USA). The Fourier-transformed infrared spectra (FT-IR) were recorded on a Perkin–Elmer Paragon® 1000 FT-IR spectrometer. The frequencies of the infrared absorption bands are expressed in terms of wavenumbers (cm^{-1}).

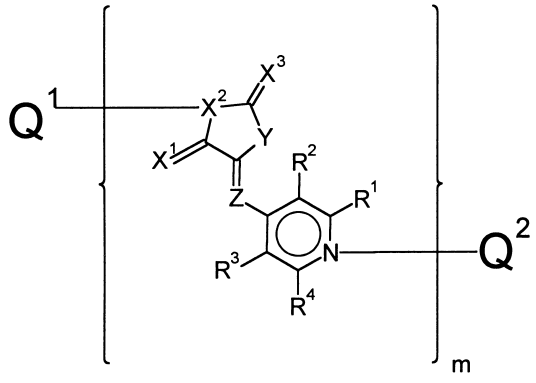

Figure 12. Example of one general formula containing the B6PR lead structure for constructing new derivatives with different substituents, specifity and antioxidant properties.

(*Z*)-5′-*O*-Phosphono-pyridoxylidenerhodanine, (*Z*)-5-[[5-hydroxy-6-methyl-3-[(phosphonooxy) methyl]-4-pyridinyl]methylene]-2-thioxo-4-thiazolidinone (2). Crude product: A stirred solution of 3.83 g rhodanine (2-thioxo-4-thiazolidinone) (28.76 mmol) in 150 mL of hot ethanol was suspended with 7.63 g of pyridoxal 5′-phosphate monohydrate (28.78 mmol). The suspension was refluxed for 20 min. After that time 150 mL of water were added, and the reaction product was refluxed for no more than 10 min. After cooling, the product was collected, washed with ethanol and dried; yield: 9.85 g orange-yellow granules without defined melting point. Purification: 9.85 g of the crude product were suspended in 610 mL of water. Then 200 mL of a saturated solution of sodium bicarbonate in water was added. The stirred red solution was titrated with 238 mL of 1.0 M hydrochloric acid. At the end of the titration the color changed from red to yellow and the free acid precipitated. The product was collected in a filter flask and dried for 48 h at a pressure of 4 mbar and a temperature of 70 °C; yield: 8.70 g (88% for this procedure, 83% for overall synthesis) yellow powder of **2** (M = 362.31 g/mol): mp 198–201 °C (dec.); ^{1}H NMR (DMSO-d_6): δ 2.42 (s, 3H, 2′-CH_3), 4.89 (d, $^3J_{^{31}P,^1H}$ = 8.0 Hz, 2H, 5′-CH_2-OPO_3H_2), 7.55 (s, 1H, 4′-CH), 7.84 (s, 1H, 6-CH); ^{1}H NMR (pyridine-d_5): δ 2.72 (s, 3H, 2′-CH_3), 5.62 (d, $^3J_{^{31}P,^1H}$ = 8.0 Hz, 2H, 5′-CH_2-OPO_3H_2), 8.36 (s, 1H, 4′-CH), 8.53 (s, 1H, 6-CH); ^{1}H NMR (D_2O) (NMR): δ 2.57 (s, 3H, 2′-CH_3), 5.06 (d, $^3J_{^{31}P,^1H}$ = 8.0 Hz, 2H, 5′-CH_2-OPO_3H_2), 7.67 (s, 1H, 4′-CH), 7.72 (s, 1H, 6-CH); ^{1}H NMR (D_2O) (NMR + UV): δ 2.57 (s, 3H, 2′-CH_3), 5.06 (d, $^3J_{^{31}P,^1H}$ = 8.0 Hz, 2H, 5′-CH_2-OPO_3H_2), 7.70 (s, 1H, 4′-CH), 7.72 (s, 1H, 6-CH); IR (KBr): 3430 (ν N-H, m), 1713 (ν C = O, s), 1213 (ν P = O, s), 1046 (ν C = S, s), 1024 (ν P = O, s); UV/VIS (H_2O): $\lambda_{max,1}$ = 232 nm [A (1%/1 cm) = 373], $\lambda_{max,2}$ = 308 nm [A (1%/1 cm) = 271], $\lambda_{max,3}$ = 353 nm [A (1%/1 cm) = 413], $\lambda_{max,4}$ = 454 nm [A (1%/1 cm) = 227]; UV/VIS (MeOH): $\lambda_{max,1}$ = 291 nm [A (1%/1 cm) = 245], $\lambda_{max,2}$ = 347 nm [A (1%/1 cm) = 489]; UV/VIS (DMSO): λ_{max} = 518 nm [A (1%/1 cm) = 98]; Fluorescence (DMSO): λ_{ex} = 490 nm: $\lambda_{em,\ max}$ = 575 nm; Fluorescence (pyridine): λ_{ex} = 490 nm: $\lambda_{em,\ max}$ = 575 nm.

Preparative synthesis of (*Z*)-5-[[5-hydroxy-6-methyl-3-[(phosphonooxy)methyl]-4-pyridinyl]methylene]-2-thioxo-4-thiazolidinone monosodium salt (4). (1) 1.93 g dry **2** (5.32 mmol) were mixed with 107 mL of 0.1 M sodium hydroxide solution. Addition of 53 mL of ethanol followed and the mixture was frozen. The precipitated crystals were filtered; yield: 1.57 g (55%) light-red needles **4a** (8½ hydrate) (M = 537.42 g/mol). Before elemental and IR analysis 340 mg of **4a** were dried for 2 days at a pressure of 0.1 mbar and a temperature of 70 °C; yield: 272 mg dark-red needles **4b**. (2) 8.7 g dry **2** (24 mmol) were mixed with 240 mL of 0.1 M sodium hydroxide

solution and the addition of 124 mL of ethanol followed. The mixture was frozen. The precipitated crystals were filtered and dried at room temperature for 2 days at a pressure of 0.1 mbar; yield: 7.55 g (73%) dark-red needles **4b**: mp 205–208 °C (dec.); IR (KBr): 3277 (ν O-H, m, broad), 1700 (ν HN-C = O, w), 1229 (ν P = O, m), 1198 (ν HN-C = S, s), 1090 (ν C = S, s), 973 (ν P-O-C, m). Anal. $C_{11}H_{10}N_2NaO_6PS_2 \times 2.5H_2O$; C 30.77% H 3.52% N 6.52%; found C 30.97% H 3.43% N 6.35%. Karl Fischer titration and elemental analysis of **4b**, in addition to theoretical considerations from X-ray structure (**4a**) pointed to 2½ hydrate **4b** ($M = 429.33$ g/mol).

X-ray analysis

Light-red crystals of **4a** (monosodium salt) were obtained from aqueous ethanol. They were stable without the mother liquor in air and were selected at room atmosphere for X-ray crystallography. The selected crystal had the dimensions $0.07 \times 0.43 \times 0.47$ mm. The structure (Fig. 2(a),(b))[6] was solved by direct methods (SHELXS-86) using 3972 unique reflections[6] (Enraf–Nonius CAD4 diffractometer with a graphite monochromator). Hydrogen atoms were included by using a riding model and anisotropic refinement (SHELXL-93) led to the agreement factors $R1 = 0.0658$ and $wR2 = 0.1642$ for 2781 reflections with $I_0 > 2\sigma(I_0)$, and to the agreement factors $R1 = 0.1006$ and $wR2 = 0.1903$ for all 3972 reflections (Table 1).[6] Six hydrogen atoms could not be located due to disorder, they are to be expected at the water molecules with O11 and O11A, and at the oxygens O4 and O4D of the phosphoric acid monoester group. The goodness-of-fit refined with F_0^2-data was 1.017.

Table 1 Crystallographic details if **4a**

Crystallographic parameter	
Empirical formula	$C_{22}H_{54}N_4Na_2O_{29}P_2S_4$
Formula weight	1074.85 g/mol
Temperature	293(2) K
Wavelength	0.71073 Å
Crystal system	monoclinic
Space group	C2/c
Unit cell dimensions	$a = 11.905(3)$ Å
	$b = 26.741(4)$ Å
	$c = 14.537(6)$ Å
	$\beta = 103.73(3)°$
Volume	4496(2) Å^3
Z (formula units per cell)	4
Density (calculated)	1.579 Mg/m^3
Absorption coefficient	0.399 mm^{-1}
$F(000)$	2224
Crystal size	$0.47 \times 0.43 \times 0.07$ mm
Θ range for data collection	2.64° to 25.00°
Index ranges	$-14 \le h \le 13$, $0 \le k \le 31$, $0 \le l \le 17$
Reflections collected	4138
Independent reflections	3972 [R(int) = 0.0229]
Absorption correction	Semi-empirical from ψ-scans
Max. and min. transmission	0.9985/0.9286
Refinement method	Full-matrix least-squares on F^2
Data/restraints/parameters	3972/25/341
Goodness-of-fit on F_0^2	1.017
Final R indices [$I > 2\sigma(I)$]	$R1 = 0.0658$, $wR2 = 0.1642$
R indices (all data)	$R1 = 0.1006$, $wR2 = 0.1903$
Largest diff. peak and hole	0.646 e/Å^{-3}/−0.458 e/Å^{-3}

Biological activities

HUT 78 test system for HIV-1 infection. The HUT 78 T lymphoma cells were infected with 100 $TCID_{50}$ of HIV-1 subtype B isolate MVP-899, a laboratory-adapted T-tropic SI strain. Tests including B6PR were performed by adding **4a** in the designated concentrations before infection at day 0.[26]

MTT mitochondrial viability assay. The HUT 78 T lymphoma cells were infected with 100 $TCID_{50}$ of HIV-1 subtype B isolate MVP-899. Tests including B6PR were performed by adding **4a** in the concentration 1 μg mL^{-1} before infection at day 0. Measurements of the mitochondrial dehydrogenase activity[8] of the HUT 78 cells were done at day six (Fig. 6) with the reagent 3-(4,5-dimethylthiazol-2-yl)-2,5-diphenyltetrazolium bromide (MTT) (Sigma Chemical Co., St Louis, MO, USA) which was measured as reduced, blue formazan at a wavelength of 650 nm.

Cancer cell line growth assay. Testing for evaluation of B6PR as potential anticancer drug was performed at the National Institutes of Health, National Cancer Institute (NCI), Bethesda, Maryland, USA, according to the published NCI criteria.[27]

Pre-B tumor cell proliferation assay. Abelson 8.1 cells[10,11] were grown in stationary suspension culture. The detailed experimental conditions and a tumor cell alkaline phosphatase assay were as described.[10]

Cultivation of macrophages and measurement of nitrite production. Murine bone-marrow-derived macrophages (BMMØ) were grown as described.[10] Nitrite production in the cell culture supernatant was measured with the Griess reagent.

S100β-specific autoreactive T cell proliferation assay. The experimental conditions were as described.[25] Proliferation was measured by [^{3}H]-thymidine incorporation into DNA. Given values are mean of three experiments not exceeding 5% relative standard deviation.

Acknowledgements

The authors would like to thank Professor Dr. Peter Hans Hofschneider, Professor Dr. Friedrich Lottspeich, Professor Dr. Dieter Oesterhelt, Professor Dr. Peter Fromherz, Professor Dr. Robert Huber and Professor Dr. Friedrich Cramer for supporting generously this work. We are greatly indebted to the National Institute of Health, National Cancer Institute (NCI), Betheseda, MD, USA, Margit Hillman and Andreas Daiber for testing, and to Manfred Heidecker for providing the fluorescence data.

References and Notes

1. (a) György, P. *Nature (London)* **1934**, *133*, 498. (b) György, P. *Biochem. J.* **1935**, *29*, 741. (c) Korytnyk, W. *Methods Enzymol.* **1979**, *62D*, 454.

2. Feigl, F. *Z. Anal. Chem.* **1928**, *74*, 380.
3. Escobar Godoy, R.; Guiraúm Pérez, A. *Analyst* **1986**, *111*, 1297; *C. A.* **1986**, *105*, 237593v; *C. A.* **1997**, *126*, 15758CS; CAS Registery No. [185195-69-1].
4. Kesel, A. J.; Urban, S.; Oberthür, W. *Tetrahedron* **1996**, *52*, 14787; *C. A.* **1997**, *126*, 59790f; *C. A.* **1997**, *126*, 15758CS; **2** CAS Registery No. [185195-66-8]; **3** CAS Registery No. [185195-67-9].
5. Kesel, A. J.; Oberthür, W. **PCT Int**. pat. **Appl. EP97 06184**.
6. ZORTEP; Zsolnai, L. *Universität Heidelberg* **1994**; SHELXS-86; Sheldrick, G. M. *Universität Göttingen* **1986**; SHELXL-93; Sheldrick, G. M. *Universität Göttingen* **1993**. Further details may be obtained from the FIZ Karlsruhe, Gesellschaft für wissenschaftlich-technische Information mbH, D-76344 Eggenstein-Leopoldshafen, Germany, on quoting the depository number CSD-408124, the names of the authors, and the journal citation.
7. Gazdar, A. F.; Carney, D. N.; Bunn, P. A.; Russell, E. K.; Jaffe, E. S.; Schechter, G. P.; Guccion, J. G. *Blood* **1980**, *55*, 409.
8. Pauwels, R.; Balzarini, J.; Baba, M.; Snoeck, R.; Schols, D.; Herdewijn, P.; Desmyter, J.; De Clercq, E. *J. Virol. Meth.* **1988**, *20*, 309.
9. Gürtler, L. *Lancet* **1996**, *348*, 176.
10. Modolell, M.; Munder, P. G. *J. Immunol. Meth.* **1994**, *174*, 203.
11. Culvenor, J. G.; Harris, A. W.; Mandel, T. E.; Whitelaw, A.; Ferber, E. *J. Immunol.* **1981**, *126*, 1974.
12. (a) Druckrey, H.; Raabe, S. *Klin. Wochenschr.* **1952**, *30*, 882. (b) Oelschläger, H.; Rothley, D.; Dunzendorfer, U. *Arzneim.-Forsch.* **1988**, *38*, 1502. (c) Schulz, P.; Bauer, H. W.; Brade, W. P.; Keller, A.; Fittler, F. *Cancer Res.* **1988**, *48*, 2867. (d) Droz, J.-P.; Kattan, J.; Bonnay, M.; Chraibi, Y.; Bekradda, M.; Culine, S. *Cancer* **1993**, *71*, 1123. (e) Robertson, C. N.; Roberson, K. M.; Padilla, G. M.; O'Brien, E. T.; Cook, J. M.; Kim, C.-S.; Fine, R. L. *J. Natl Cancer Inst.* **1996**, *88*, 908.
13. Fauci, A. S. *Nature* **1996**, *384*, 529.
14. MacMicking, J. D.; Nathan, C.; Hom, G.; Chartrain, N.; Fletcher, D. S.; Trumbauer, M.; Stevens, K.; Xie, Q.-W.; Sokol, K.; Hutchinson, N.; Chen, H.; Mudgett, J. S. *Cell* **1995**, *81*, 641.
15. Adamson, D. C.; Wildemann, B.; Sasaki, M.; Glass, J. D.; McArthur, J. C.; Christov, V. I.; Dawson, T. M.; Dawson, V. L. *Science* **1996**, *274*, 1917.
16. Frey, C.; Narayanan, K.; McMillan, K.; Spack, L.; Gross, S. S.; Masters, B. S.; Griffith, O. W. *J. Biol. Chem.* **1994**, *269*, 26083.
17. (a) Kesel, A. J.; Polborn, K.; Hillmann, M.; Klinkert, W. E. F.; Modolell, M.; Oberthür, W. XVIIth International Winter Meeting, Swiss Society of Neuropathology, St. Moritz, Switzerland, 14-18th March 1998. (b) Bredt, D. S.; Snyder, S. H. *Annu. Rev. Biochem.* **1994**, *63*, 175. (c) Griffith, O. W.; Stuehr, D. J. *Annu. Rev. Physiol.* **1995**, *57*, 707.
18. Shu, Z.; Jung, M.; Beger, H.-G.; Marzinzig, M.; Han, F.; Butzer, U.; Bruckner, U. B.; Nussler, A. K. *Am. J. Physiol.* **1997**, *273*, G1118.
19. Marzinzig, M.; Nussler, A. K.; Stadler, J.; Marzinzig, E.; Barthlen, W.; Nussler, N. C.; Beger, H. G.; Morris, Jr. S. M.; Brückner, U. B. *Nitric Oxide* **1997**, *1*, 177.
20. Kröncke, K.-D.; Fehsel, K.; Kolb-Bachofen, V. *Nitric Oxide* **1997**, *1*, 107.
21. The Neurobiology of NO· and ·OH; Chiueh, C. C.; Gilbert, D. L.; Colton, C. A. Eds; N. Y. Acad. Sci.: New York, 1994.
22. López-Moratalla, N.; González, Á.; Aymerich, M. S.; López-Zabalza, M. J.; Pío, R.; de Castro, P.; Santiago, E. *Nitric Oxide* **1997**, *1*, 95.
23. Bagasra, O.; Michaels, F. H.; Zheng, Y. M.; Bobroski, L. E.; Spitsin, S. V.; Fu, Z. F.; Tawadros, R.; Koprowski, H. *Proc. Natl Acad. Sci. USA* **1995**, *92*, 12041.
24. Wekerle, H.; Kojima, K.; Lannes-Vieira, J.; Lassmann, H.; Linington, C. *Ann. Neurol.* **1994**, *36*, 47.
25. Kojima, K.; Reindl, M.; Lassmann, H.; Wekerle, H.; Linington, C. *Intern. Immunol.* **1997**, *9*, 897.
26. Gürtler, L. G.; Hauser, P. H.; Eberle, J.; von Brunn, A.; Knapp, S.; Zekeng, L.; Tsague, J. M.; Kaptue L. *J. Virol.* **1994**, *68*, 1581.
27. Grever, M. R.; Schepartz, S. A.; Chabner, B. A. *Seminars in Oncology* **1992**, *19*, 622.